Table 1 Experimental rolling moment coefficient

Configuration	Rolling moment coefficient, C_l
A	4.0×10^{-6}
B	6.7×10^{-6}
C	5.3×10^{-6}

fins, thus acting to oppose the driving forces. The situation was corrected by sweeping the fin trailing edges 30°.

During the tests the cone base pressure was measured inside the model to help insure that there were no significant interference effects and that the flow was expanding in a normal manner around the cone-base corner. The ratio of the model base pressure to the tunnel test-section ambient pressure was about 0.20, and comparisons of the measured base-pressure coefficient with other sources of data indicate that the flow in the recirculation zone was not abnormal.[10]

Flight Dynamics

The conditions that produce roll resonance during ballistic flight are functions of the trajectory parameters and of the mass and aerodynamic properties of the vehicle. The criterion for the occurrence of steady roll resonance in circular motion with small angle of attack derived by Vaughn[7] is

$$(2I_y^{1/2}/I_x)(C_{N_\theta}A/x_{c.p.})^{1/2}(q_\infty^{3/2}/\dot{q}_\infty)(\theta - \alpha_t)y_0 \geq 1 \quad (1)$$

where y_0 is the lateral displacement of the roll axis from the center of mass, and α_t is the out-of-plane aerodynamic trim angle. If Eq. (1) is satisfied, then roll control is necessary, and the magnitude of the required control moment may be estimated by including the rolling moment in the original equation of motion and rederiving the aforementioned criterion. The final result is

$$|C_l| \geq |C_{N_\theta}(\theta - \alpha_t)(y_0/d) - (I_x/I_y^{1/2})(C_{N_\theta}x_{c.p.}/S)^{1/2}(\dot{q}_\infty/q_\infty^{3/2})(2d^{-1})| \quad (2)$$

where C_l is the dimensionless control moment coefficient. The first term on the right-hand side of the equation is the moment coefficient due to configurational asymmetry, and the other term is due to aerodynamic, inertia, and trajectory effects. The experimental rolling-moment coefficients for the three impeller configurations are shown in Table 1.

Although the maximum possible rolling moment has not been determined in the tests discussed here, an indication of the amount of configurational asymmetry that can be controlled by an optimized impeller design may be obtained by considering the capability of the existing impeller configurations at zero angle of attack. For that purpose it is sufficient to consider only the first term in Eq. (2). By way of example, for a 10° half-angle cone with an 0.1° trim angle in Newtonian flow, the maximum out-of-plane, center-of-mass displacement that can be tolerated for configuration B is $y_0/d = (6.7 \times 10^{-6})(57.3)/(1.96 \times 0.1) = 2.0 \times 10^{-3}$, or 0.048-in. for a 1-ft-radius cone. The inclusion of the remaining term in Eq. (2) will normally increase the permissible configuration asymmetry. However, this increase is not significant for conventional re-entry vehicles unless the trajectory is particularly steep or the dynamic pressure is small. By examining Eq. (2), it may be seen that vehicles with larger configurational asymmetries, and vehicles that are smaller in size, require proportionally larger control moments; further, for $\theta \geq \alpha_t$, an increase in the total angle of attack necessitates a larger control moment.

The characteristics of existing ablation materials and current manufacturing techniques may not be sufficient to maintain the required configurational asymmetry for the assumed vehicle if the ballistic factor is large. Therefore, in practice, either an improved impeller design to provide more control torque or a larger vehicle may be required.

References

[1] Maple, C. G. and Synge, J. L., "Aerodynamic Symmetry of a Projectile," *Quarterly of Applied Mathematics*, Vol. IV, No. 4, Jan. 1949, pp. 345–366.

[2] Nelson, R. L., "The Motions of Rolling Symmetrical Missiles Referred to a Body-Axis System," TN 3737, Nov. 1956, NASA.

[3] Murphy, D. H., "Free Flight Motion of Symmetric Missiles," Rept. 1216, July 1963, Ballistic Research Labs., Aberdeen, Md.

[4] Glover, L. S., "Effects on Roll Rate of Mass and Aerodynamic Asymmetries for Ballistic Re-Entry Bodies," *Journal of Spacecraft and Rockets*, Vol. 2, No. 2, March-April 1965, pp. 220–225.

[5] Pettus, J. J., "Persistent Re-Entry Vehicle Roll Resonance," AIAA Paper 66-49, New York, 1966.

[6] Platus, D. H., "A Note on Re-Entry Vehicle Roll Resonance," *AIAA Journal*, Vol. 5, No. 7, July 1967, pp. 1348–1350.

[7] Vaughn, H. R., "Boundary Conditions for Persistent Roll Resonance on Re-Entry Vehicles," *AIAA Journal*, Vol. 6, No. 6, June 1968, pp. 1030–1035.

[8] Barbera, F. J., "An Analytical Technique for Studying the Anomalous Roll Behavior of Ballistic Re-Entry Vehicles," AIAA Paper 69-103, New York, 1969.

[9] Lockman, W. K., "Free-Flight Base Pressure and Heating Measurements on Sharp and Blunt Cones in a Shock Tunnel," *AIAA Journal*, Vol. 5, No. 10, Oct. 1967, pp. 1898–1900.

[10] Cassanto, J. M., Rasmussen, N. S., and Coats, J. D., "Correlation of Measured Free Flight Base Pressure Data for $M = 4$ to $M = 19$ in Laminar and Turbulent Flow," AIAA Paper 68-699, Los Angeles, Calif., 1968.

Mission Analysis Models for Power-Limited Systems

ROBERT V. RAGSAC*
United Aircraft Research Laboratories, East Hartford, Conn.

IN constructing some mission models for power-limited interplanetary spacecraft systems, the levels of reality employed in characterizing the vehicle system's constituent subsystems and operational constraints are important. This Note discusses some systems analysis models for the purpose of evaluating flight concepts, propulsion mixes and power system performance.

One major guideline was to construct a separate model for each flight mode (not mission); i.e., single-stage operation or mixed-thrust operation, both for a) a given range of powerplant specific mass α_W, b) a given α_W and powerplant mass m_W, and c) given m_W, α_W, and spacecraft gross mass m_0. This approach was employed to gain experience in the synthesis and use of the models and to apply this insight for the development of slightly more general models which allow added refinement and sophistication. The system characterization is a set of equations which describe the net spacecraft mass fraction μ_L, or mass m_L, in terms of the high- and low-thrust propulsion parameters, the trajectory requirements and flight mode. For example, for a single-stage electric propulsion system operating through three gravitational fields,

$$\mu_L = \left[1 + \frac{\alpha_W}{2\eta}\frac{(J_D + J_H + J_C)}{\mu_W}\right]^{-1} - \mu_W \quad (1)$$

Presented at the AIAA 7th Electric Propulsion Conference, Williamsburg, Va., March 3–5, 1969 (no paper number; published in bound volume of meeting papers); submitted April 25, 1969; revision received August 4, 1969.

* Senior Research Engineer.

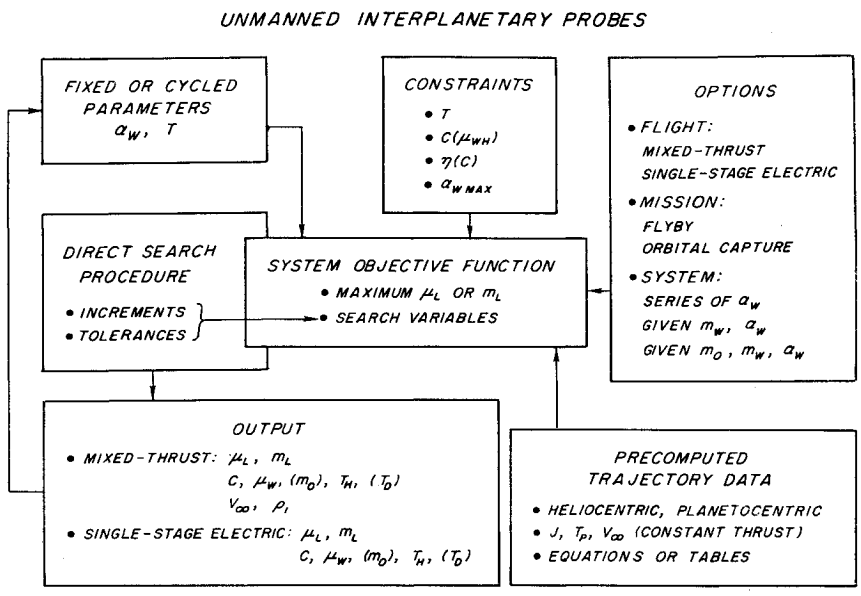

Fig. 1 Schematic of developed mission analysis model.

where J_D, J_H, and J_C are the low-thrust trajectory requirements for earth departure spiral, heliocentric transfer, and planetary capture spiral, respectively, η is the thruster efficiency, and μ_W is the powerplant fraction. If this flight mode were to include a high-thrust system which operates after a departure spiral but before the start of the heliocentric phase, then

$$\mu_L = \left(1 - \frac{\gamma_D{}^2}{\eta\mu_{WH}\mu_\Delta}\right)\mu_\Delta\left[\left(1 + \frac{\gamma_H{}^2 + \gamma_C{}^2}{\eta\mu_{WH}}\right)^{-1} - \mu_{WH}\right] \tag{2}$$

where $\gamma^2 = \alpha_W J/2$ and the subscripts D, H, and C indicate the low-thrust trajectory requirements for the departure spiral, heliocentric transfer and capture spiral, respectively, μ_{WH} is the powerplant fraction at the initiation of the heliocentric phase, and μ_Δ is the payload to gross mass fraction of the high-thrust stage.

The low-thrust propulsion system parameters enter into the formulation through α_W and η, the latter being some function of the exhaust velocity C (or specific impulse I_{sp}). Note that the masses of the thrusters, propellant tanks and tie-in structure are not accounted for; i.e., the level of detail in the system description is restricted to preliminary evaluations. Nevertheless, the description of the flight mode is fairly detailed in terms of the trajectory data.

The high-thrust system is represented by μ_Δ, which is a simplification of the stage masses;

$$\mu_\Delta = (1 - \mu_h\beta)/(1 - \beta)\mu_h \tag{3}$$

where $\mu_h = \exp(\Delta V/I_{sp}g)$, β is the step inert mass fraction (constant), ΔV is the impulsive velocity requirement.

The computer program for the low-thrust heliocentric trajectory model[1] solves the variational equations for maximizing the net mass fraction in a fixed-time, constant-power, constant-exhaust-velocity, power-limited, three-dimensional heliocentric trajectory. For the purposes of the system model only, J_H and heliocentric powered time are utilized as a function of time for either flyby or capture. Since high-thrust operation at departure is assumed, J_H must also be given as a function of hyperbolic excess speed V_∞, at the initial boundary of the heliocentric trajectory. The planetocentric spirals (elliptic for departure and circular spiral for capture) are computed from straightforward equations.[2] The optimization problem, in general, is to determine the time for each trajectory phase, V_∞, μ_W, and the radius r_1, for applying the high thrust, all of which maximize μ_L. A numerical direct search procedure was used.[3]

It was found expedient to precompute all of the heliocentric low-thrust data as a function of trip time T and V_∞ for both planetary flyby and rendezvous missions for two reasons: 1) the trajectory model,[1] although computationally fast in relation to other equivalent programs, is not suited to being directly coupled to and controlled by the search procedure, which requires a solution from the trajectory program at each trial step; and 2) convergence to some trajectories, for example those with very short transfer times, cannot be achieved without special iterative starting techniques. Therefore, the precomputed trajectory data were thus handled either by curve fitting (errors were <1%) the various functions or by storing the data tables and employing a nonlinear interpolation technique. A sampling of the heliocentric and planetocentric trajectory data as used in a simplified single-stage, low-thrust system analysis model is presented in Ref. 2.

The preferred arrangement would be to develop a program that provides a complete solution of a mixed-thrust trajectory in much less than a second of machine time. A step in this direction was achieved by Johnson for variable thrust trajectories.[4] Other than computational speed, probably the next major goal of trajectory model development should be the computation of the over-all, composite low-thrust trajectory which includes the position and velocity transition effects between gravitational fields. This type of trajectory program could be used to verify or improve current approximation techniques (e.g., see Refs. 5 and 6).

The vehicle system was characterized in nondimensional form in order to 1) obtain preliminary information on a broad range of flight modes and missions, and 2) to pick those apparent favorable applications for a more detailed system study. The first step requires simplifying assumptions for defining μ_L and characterizing the high thrust stage. Equations (1) and (2) are based on the simplest definition for net mass fraction; namely, the difference between the terminal mass fraction and powerplant fraction. This preliminary level of system detail ignores the mass of the thrusters, propellant tanks, and tie-in structure. These masses could be accounted for by redefining the powerplant mass to include estimates for the additional masses.

The high-thrust stage mass effects were cast into nondimensional form by using β to represent the ratio of the step inert mass to the inert mass plus propellants. It is assumed that β is essentially constant, Eq. (3), regardless of the velocity increment the high-thrust stage is to produce. Actually β depends on the propellant mass.

Because most models developed have as their initial objective the preliminary evaluation of system concepts and missions, the mixed-thrust system model should use a rather

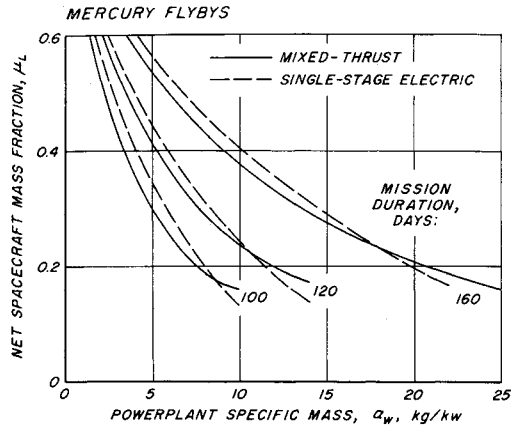

Fig. 2 Sample results from mission model of Fig. 1.

simple definition of μ_L but should account in fair detail for the dynamic aspects of the flight. Changes in the flight profile, e.g., terminal parking orbit radius, location and magnitude of the high-thrust impulse, type of low-thrust departure spiral, etc., usually have greater effects on the performance than variations in the mass breakdown of the spacecraft.

What Elements of Reality?

The level of reality or detail that one builds into a mission model is guided largely by the intended use of the results. In practice, efforts to refine a model so it realistically portrays the performance of the vehicle system as it executes an "actual" trajectory are directed toward three broad elements: 1) the description of the vehicle's subsystems, 2) the characterization of the flight profile, and 3) the operational constraints on the vehicle.

The net mass of the vehicle becomes closer to useful payload when it is redefined as the terminal mass less the mass of the powerplant, thrusters, tanks, and structure of the low-thrust system. The tanks may be accounted for by defining ρ as the ratio of the propellant mass to the mass of the propellant plus tank, and the tie-in and miscellaneous structure may be considered as a fraction σ of the total inert mass of the electric propulsion system. The thruster mass depends, generally, on the input power and jet velocity it produces; a thruster specific mass α_F, usually considered as a function of I_{sp}, may be defined as the ratio of thruster mass to input power. Hence, for a single-stage electric system only, the net mass fraction (now more nearly useful payload) is

$$\mu_L = 1 - \frac{1+\sigma}{\rho}\left[1 - \left(1 + \frac{\gamma^2}{\eta\mu_W}\right)^{-1}\right] - (1+\sigma)\left(1 + \frac{\alpha_F}{\alpha_W}\right)\mu_W \quad (4)$$

Now the optimization must account for the dependence of thruster efficiency and specific mass on I_{sp}. Note that the thruster characterization does not represent any particular thruster in terms of power and thrust level, although it does represent a given type of design. The optimization approach would be quite different if a particular thruster, complete with mass, power, and thrust level, was given.

If more detail is desired in modeling the high-thrust system, it practically becomes necessary to abandon the nondimensional approach of Eq. (3), since β depends on the mass of the high-thrust propellant and minimum inert mass requires optimizing the impulsive thrust-to-mass ratio. The approximation in Eq. (3), however, has been found to be reasonable.

An accurate characterization of the flight profile usually centers on accounting for n-body effects. Based on the background accumulated so far it appears that accurate, simplified approximation techniques are most useful mainly because of the machine time. The results of n-body studies would be useful either for producing information for analytical curve fits or for verifying and updating present analytical approximations. At present, it appears unreasonable to integrate directly a sophisticated, physically exact trajectory model into a mission model, if the study objectives are mission planning and systems evaluation.

The last broad element into which realistic performance may be injected is the actual statement of the vehicle's operating constraints or limitations. Vehicle operation is interpreted to consist of three cases: 1) operation with a "free" powerplant, i.e., specified only by α_W, 2) given m_W and power output, and 3) condition 2 along with fixed m_0. Hardware performance includes three cases: 1) the thruster is specified only through the dependence of η and α_F on I_{sp}, 2) the thruster mass, input power, and thrust level are given, and 3) a specific type of high-thrust stage is to be used. These classifications point out the fact that in a mission performed by an electrically-propelled vehicle, most, if not all, of the subsystems will have fixed operating characteristics not necessarily optimum in relation to the entire vehicle and mission. A model should reflect such system realities to allow the analysis of systems "off the shelf" or projected for the mission time period. This flexibility influences not only the characterixation of μ_L but also the variables remaining for optimization. As an example, if the powerplant mass and power output were fixed, then instead of Eq. (2) the equation to be maximized is

$$\frac{m_L}{m_W} = \left[\frac{1}{\mu_\Delta}\left(\frac{m_W}{m_0} + \frac{\gamma_D^2}{\eta}\right) + \frac{\gamma_H^2 + \gamma_C^2}{\eta}\right]^{-1} - 1 \quad (5)$$

where, in effect, m_0 becomes a search variable. If m_0 were also specified, e.g., by a given surface launch booster, then m_W/m_0 is treated as a constant.

An important member of the model which actually cannot be classified with either the system characterization or the trajectory model is the approximation required to uncouple the dependence of the trajectory steering program on the vehicle system parameters. This approximation is based on the observation that given any reference fixed-time, constant-thrust trajectory over which J has been minimized, a recalculation of the identical trajectory using any other values for μ_W and α_W will yield practically the same J and average thrust acceleration.[7] A relationship is therefore derived between C and μ_{WH} which must be satisfied at each search step in the optimization procedure,

$$\begin{aligned} \bar{a}\alpha_W C &= 2\eta\mu_{WH} + \gamma_H^2 \quad \text{AM} \\ \bar{a}\alpha_W C &= 2\eta\mu_{WH}\left(1 + \frac{\gamma_H^2}{\eta\mu_{WH}}\right)^{1/2} \quad \text{GM} \end{aligned} \quad (6)$$

where AM and GM are the arithmetic mean and geometric mean definitions for average thrust acceleration $\bar{a}$;

$$\bar{a} = \frac{a_0 + a_1}{2} \quad \text{AM}, \qquad \bar{a} = (a_0 a_1)^{1/2} \quad \text{GM}$$

where a_0 and a_1 are the initial and final thrust accelerations, respectively, of the reference heliocentric trajectory. Equation (6) states that at each μ_{WH}, and trip time, the best exhaust velocity to use is that which maximizes μ_L on the heliocentric portion of the entire flight. Equation (6) is convenient for mission analysis and is advantageous in developing the corresponding model. However, it is strictly an approximation and does not precisely reproduce the actual trajectory J, especially at very low μ_{WH}. The development of more accurate approximation methods is highly desirable.

A schematic of the mission analysis model is shown in Fig. 1. After flight, mission, and system options are chosen, the total mission duration T is selected and μ_L is maximized for each value of α_W. The constraints are: $C(\mu_{WH})$, which rep-

resents Eq. (6) or its equivalent; $\eta(C)$; and $\alpha_{W,max}$, an equation which estimates, at each solution, the value of α_W which will produce zero net mass fraction. The search variables are generally μ_W, T_H (heliocentric trip time), T_D (departure trip time), V_∞, and r_1 (radius of impulsive thrust application). Figure 2 presents a typical set of results.

Some General Considerations

As experienced here, the following items have major effects on the structure and formulation of the model: 1) purpose of the model, 2) level of detail required, 3) number of flight profiles and system variations, 4) the submodels available, and 5) the choice of optimization techniques.

Generally, it is advantageous in terms of machine time and convergence to employ approximations for the trajectory requirements in the different flight modes. Further, approximation techniques for representing the interrelationship between the trajectory and the vehicle are useful in permitting separate and distinct subroutines for each.

If the numerical procedure or, in fact, the solution of any set of equations within the model requires an iterative procedure with input starting guesses, it is most efficient to specify a system parameter (e.g., α_W) as the principle variable for a given set of system and flight conditions. In this way starting solutions for both search variables and other parameters are generated internally, and information will be available for various α_W's should the particular desired α_W (or some lower value) encounter nonconvergence or yield unacceptable net mass fractions.

A task which merits intensive analysis is the inclusion of a probabilistic characterization of the electric propulsion system's probable degradation with time due to component failure. Computer programs are needed for optimizing heliocentric, power-limited, constant-thrust trajectories with power output varying, preferably, as a function of both time and position. Reference 8 includes an initial attempt at introducing power system reliability aspects into mission studies.

A compilation of the known low-thrust system and flight mode concepts should be made in order to develop a common basis of comparison for the many studies and mission models yet to come.

References

[1] Van Dine, C. P., "Extension of the Finite-Difference Newton-Raphson Algorithm to the Simultaneous Optimization of Trajectories and Associated Parameters," AIAA Paper 68-115, New York, 1968.

[2] Ragsac, R. V., "Trajectory Requirements and Performance Computations of Single-Stage Electrically Propelled Space Vehicles," Paper 68-106, 1968, AAS.

[3] Hooke, R. and Jeeves, T. A., "Direct Search Solution of Numerical and Statistical Problems," *Journal of the Association of Computing Machinery*, Vol. 8, 1961, pp. 212–223.

[4] Johnson, F. T., "Approximate Finite-Thrust Trajectory Optimization," Paper 68-080, 1968, AAS.

[5] Fimple, W. R. and Edelbaum, T. N., "Applications of SNAP-50 Class Power-plants to Selected Unmanned Electric Propulsion Missions," AIAA Paper 64-194, Wichita, Kansas, 1964.

[6] Melbourne, W. G. and Sauer, C. G., Jr., "Performance Computations with Pieced Solutions of Planetocentric and Heliocentric Trajectories for Low-Thrust Missions," *Jet Propulsion Laboratory Space Programs Summary No. 37–36*, Vol. IV, Pasadena, Calif., 1965.

[7] Melbourne, W. G. and Sauer, C. G., "Payload Optimization for Power-Limited Vehicles," *Progress in Astronautics and Aeronautics: Electric Propulsion Development*, Vol. 9, edited by E. Stuhlinger, Academic Press, New York, 1962, pp. 617–645.

[8] Gitlow, B., Schmitt, J. W., and Ragsac, R. V., "Rankine Cycle Powerplant Characteristics for Electric Propulsion Manned Mars Mission," AIAA Paper 66-894, Boston, Mass., 1966.

Dimensionless Products of Parachute Inflation

KENNETH E. FRENCH*
Lockheed Missiles & Space Company, Sunnyvale, Calif.

Nomenclature

D_0 = parachute constructed diameter, m or ft
F_0 = parachute opening shock, N or lb
f_i = symbol denoting functional relationship (i = 1,2)
g = acceleration of gravity, m/sec² or ft/sec²
M = total system mass, kg or slug
q_s = dynamic pressure at time of full line stretch, N/m² or lb/ft²
S_0 = parachute reference drag area, m² or ft² ($= \frac{1}{4}\pi D_0^2$)
t_f = parachute inflation time, sec
v_s = system velocity at time of full line stretch, m/sec or ft/sec
θ = average flight-path angle during inflation, deg or rad
ρ = atmosphere mass density, kg/m³ or slug/ft³

Introduction

As noted previously,[1,2] dimensional considerations indicate that incompressible-flow parachute inflation may be characterized by the dimensionless products

$$F_0/q_sS_0 = f_1[(\rho D_0^3/M), (gD_0 \sin\theta/v_s^2)] \quad (1)$$

and

$$v_st_f/D_0 = f_2[(\rho D_0^3/M), (gD_0 \sin\theta/v_s^2)] \quad (2)$$

In Eqs. (1) and (2), F_0 and t_f are the variables of interest. Methods or formulas are available for the calculation of t_f for some types of parachute. These methods encompass the "infinite mass" case,[3,4] in which system velocity remains constant during inflation, and certain ranges of test conditions.[5] Methods are also available for calculation of F_0, but are rather cumbersome to apply. None of the available methods indicate the tolerances to be expected in the calculated variable under actual flight test conditions.

Equations (1) and (2) suggest that an appreciation of the dispersion to be encountered in the parachute inflation process could be obtained by plotting F_0/q_sS_0 vs v_st_f/D_0 from test data. Such a plot would also provide a useful cross-check on (or short-cut to) methods that calculate F_0 based on an initial calculation of t_f.

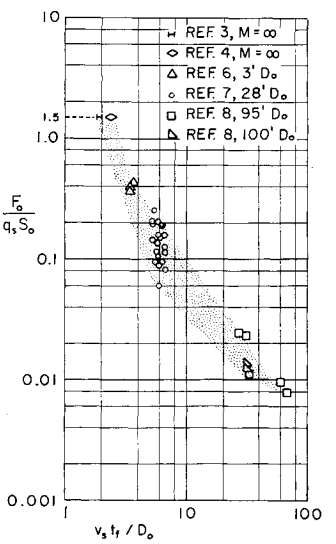

Fig. 1 F_0/q_sS_0 vs v_st_f/D_0 for various parachutes.

Received July 14, 1969.
* Staff Engineer. Associate Fellow AIAA.